TECHNICAL UNIVERSITY OF CLUJ-NAPOCA

ACTA TECHNICA NAPOCENSIS

Series: Applied Mathematics, Mechanics, and Engineering
Vol. 67, Issue Special II, April, 2024

DRILLING PERFORMANCE ANALYSIS OF STRUCTURAL ALUMINIUM ALLOY USING THE TAGUCHI METHOD

Anastasios TZOTZIS, Nikolaos EFKOLIDIS, Athanasios MANAVIS, Panagiotis KYRATSIS

Abstract: *Drilling of structural aluminum alloys (AA) is one of the most frequently applied processes in the industry. This study utilizes a Taguchi L9 orthogonal array, to investigate the influence of three key machining parameters (cutting speed, feed and tool diameter), on the thrust force and cutting torque induced during drilling of Al6082 T6 temper with coated, carbide tools. The set of the 9 experiments was carried out on a CNC machine, whereas the desired output was measured with a rotational dynamometer. In addition, a data acquisition system was used to facilitate the output data collection. The analysis revealed that the tool diameter is the variable that affects the most, both output parameters, followed by the feed. Furthermore, the optimal cutting conditions were identified, with the minimization of the cutting forces and torque in mind.*

Key words: *Thrust force, Cutting torque, Al6082-T6, Taguchi, L9 orthogonal array, Carbide drilling.*

1. INTRODUCTION

Despite the advent of numerous novel lightweight materials in the recent years, aluminium alloys (AA) are still considered as one of the top choices for the industry. Therefore, literature contains a number of studies related to the machining of AA, especially drilling, which is constantly updated.

Veiga et al [1] studied the chip formation process during low frequency assisted drilling of stacked Al7075, as an alternative to conventional drilling and peck drilling. Kimmelmann et al [2] examined the burr formation mechanisms in CFRP-aluminium stacks, at the point of the bit exit. Tzotzis et al [3] presented a combined statistical and Finite Element (FE) model of the Al7075-T6 drilling with solid carbide tools, in three dimensions. Bharatish et al [4] investigated the laser drilling of Al6065 plates deposited with alumina, in terms of the entrance and exit hole circularity. The work by Xiang et al [5] presented findings on the micro-mechanisms involved in the tool wear, during diamond drilling of SiCp/Al6063 composites. Similar studies [6–8], implemented experimental work, statistical analysis and FE modelling, to examine critical drilling characteristics such as cutting forces and torque. These two parameters are proven indexes to measure the required machining power and examine the tool wear.

Due to the fact that most AA drilling studies that exist in the literature, focus on characteristics such as hole circularity, chip and burr formation, surface roughness, material removal rate, as well as tool wear, the present work aims to contribute towards the investigation of the force and torque generation induced during the process. Moreover, it focuses on structural aluminium and specifically on one of the latest additions in the 6000 series, namely 6082. The specific material tends to replace the 6061 alloy in many applications, such as heating systems, train decks, structural frames, trusses, food barrels and more.

2. MATERIAL AND METHODS

2.1 Experimental work

A set of nine “through hole” drilling tests were performed with a HAAS VF-1 CNC machine, according to the design given by a Taguchi L9-orthogonal array, with respect to the three machining parameters chosen and the three levels for their values. The selected machining conditions were the tool diameter, the cutting

speed and the feed rate, as shown in Table 1. These parameters are typical when assessing drilling of AA, such as the one studied in the present paper. Specifically, the T6 temper of the AA6082 was considered. The most basic mechanical properties of the material is shown in Table 2.

Table 1

Machining parameters and their levels.

Levels	V_c (m/min)	f (mm/rev)	D (mm)
+1	150	0.25	12
0	100	0.20	10
−1	50	0.15	8

Table 2

Al6082-T6 properties.

Density (kg/m³)	2700
Hardness (Vickers)	95
Poisson's ratio	0.33
Ultimate tensile yield strength (MPa)	330
Tensile yield strength (MPa)	270
Modulus of elasticity (GPa)	70
Fatigue strength (MPa)	95
Shear modulus (GPa)	26

Catalogue number	D (mm)	d (mm)	L (mm)	l (mm)
12030800	8	8	79	41
12031000	10	10	89	47
12031200	12	12	102	55

Fig.1. The geometrical characteristics of the carbide drills

Regarding the output parameters, both thrust force and cutting torque were examined. First, the thrust force is considered to be an index of the material's machinability, whereas the cutting torque is usually linked to the machine power requirements. Therefore, the investigation of these parameters, probably provide useful insight when considering the drilling of AA. To collect the output data, the 4-component Kistler 9123 revolving dynamometer was utilized, coupled with an equivalent data acquisition system comprising of a charge amplifier and a data acquisition card.

The through holes were performed with carbide, TiAlN coated tools, according to the range of values recommended by the manufacturer. The designation numbers for the identification of the tools are as follows: 12030800, 12031000 and 12031200. Finally, Figure 1 illustrates the morphology of the used two-flute, twist drills, with point angle equal to 140°. It is noted that the selected tool series, corresponds to a set of tools with decimal drilling diameter, covering a total of 41 drills, as shown in the manufacturer's catalogue.

Additionally, a beam of a semi-synthetic cooling fluid solution was directed to the machining area, to facilitate the cooling process during drilling.

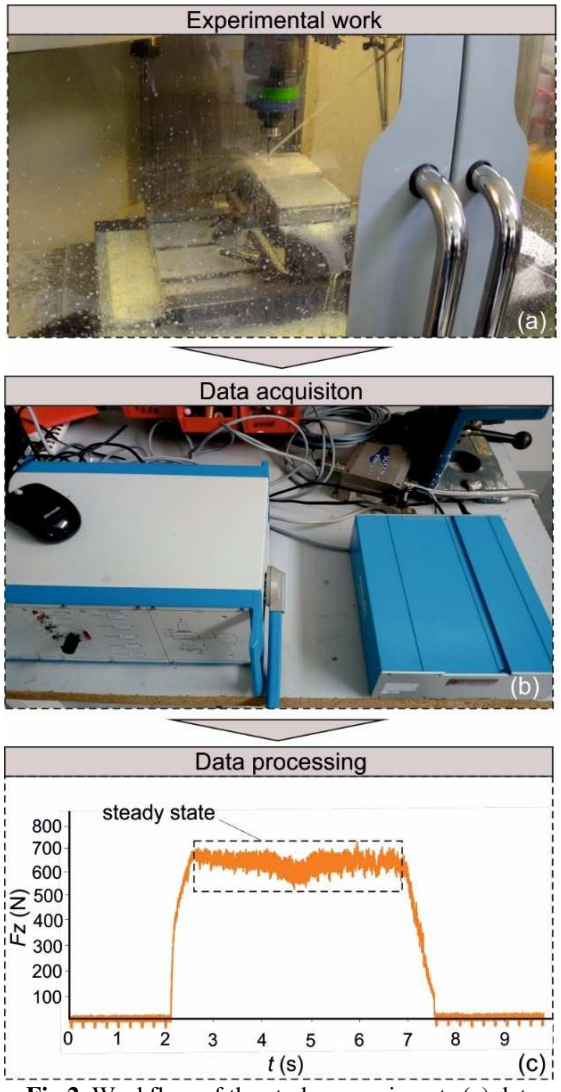

Fig.2. Workflow of the study: experiments (a) data acquisition (b) and data processing (c)

Figure 2 depicts the complete process of a sample experiment. In particular, Figure 2a was captured during the experimental phase, Figure 2b shows the data acquisition equipment and Figure 2c illustrates the acquired force versus time diagram for the specific experiment, the points of which were generated with the DynoWare software. The sample test corresponds to the following conditions: Ø10 tool, cutting speed V_c=50m/min and feed rate f=0.15mm/rev.

2.2 Taguchi L9 design

The design of the experiments was done by utilizing the L9-orthogonal array. The Taguchi method is widely implemented in similar studies [9–11], involving multiple parameters that affect a machining process. Through this method, the variation of a process is reduced significantly, leading this way to a robust design. Table 3 presents the design of the experiments according to this method, for the three cutting parameters and levels applied to the study.

Table 3

The Taguchi L9 design.

Run	V_c	f	D
1	50	0.15	8
2	50	0.20	10
3	50	0.25	12
4	100	0.15	10
5	100	0.20	12
6	100	0.25	8
7	150	0.15	12
8	150	0.20	8
9	150	0.25	10

3. RESULTS AND FINDINGS

With the completion of the experiments, the results for both the force and torque were acquired after a standard processing with spreadsheet software. Particularly, they were derived based on the calculated mean value of the steady state. The region where the generated results present a reasonable fluctuation and at the same time maintain a constant value, represents the steady state. Table 4 includes the results for both the thrust force F_z and the cutting torque M_z, according to the run order of the experiments. Additionally, it contains the signal to noise (S/N) ratios for both output parameters, based on the "smaller is better" approach. Lower values of thrust force lead to lighter tool wear and hence, reduced manufacturing cost. Moreover, thrust force is directly related to the generated surface roughness. Similarly, lower values of cutting torque, usually affect the power consumption positively. Specifically, lower torque means less machine power requirements, therefore contributing towards the cost reduction.

Table 4

The acquired output results and the equivalent S/N ratios.

Run	F_z	*S/N ratio*	M_z	*S/N ratio*
1	548	−54.7756	2.40	−7.6042
2	813	−58.2018	3.86	−11.7317
3	1348	−62.5938	6.60	−16.3909
4	784	−57.8863	3.16	−9.9937
5	1277	−62.1238	5.84	−15.3283
6	731	−57.2783	2.95	−9.3964
7	1167	−61.3414	4.86	−13.7327
8	594	−55.4757	2.63	−8.3991
9	1014	−60.1208	3.99	−12.0195

Each experiment was replicated three times and the mean value for both output parameters were calculated, in order to increase the reliability of the dataset. The S/N ratios represent the ratio between the desirable values (signal), for instance the mean value of the output, and the undesirable values (noise), which usually is the square deviation of the output. Thus, the S/N ratio is essentially the ratio of the mean value to the square deviation, and for this case were calculated with Equation 1.

$$S/N = -10\log\left(\frac{\sum y_i^2}{n}\right) \qquad (1)$$

3.1 Analysis of the dataset

The calculation of the S/N ratios revealed the significance of each one of the cutting factors involved in the study. Tables 5 and 6 present the ranking of the tool diameter, feed rate and cutting speed, in terms of their influence on the generated thrust force and torque respectively.

According to the difference between the maximum and the lowest mean value for each one of the factors, the tool affects the most both responses, followed by the feed rate.

Table 5

Mean values of F_z according to each factor level.

Level	V_c	f	D
1	903.0	833.0	624.3
2	930.7	894.7	870.3
3	925.0	1031.0	1264.0
Delta	27.7	198.0	639.7
Rank	3	2	1

Table 6

Mean values of M_z according to each factor level.

Level	V_c	f	D
1	4.287	3.473	2.660
2	3.983	4.110	3.670
3	3.827	4.513	5.767
Delta	0.460	1.040	3.107
Rank	3	2	1

By checking the delta value, it is evident that the influence of the tool on both outputs, is approximately triple compared to the influence induced by the feed. On the other hand, the effect generated by the cutting speed is much lower than the other two parameters, especially when considering the thrust force.

3.2 Model validation

The Analysis of Variance (ANOVA) was utilized for the examination of the statistical significance of the factors, as well as the goodness-of-fit, with the confidence level set to 95% [12–14]. Tables 7 and 8 present the analysis results for F_z and M_z accordingly. DF denotes the degrees of freedom of each factor, SS is the sum of squares and MS the mean squares.

The examination of the p-value of each of the terms, revealed their significance. It is pointed out that every factor with a p-value lower than 0.05, which derives from the confidence level, presents an increased contribution. Therefore, the tool seems to have the most significant effect on both the output factors, as expected, verifying the analysis of the dataset. Subsequently, the feed rate illustrates strong influence, whereas the cutting speed cannot be considered as significant.

Table 7

ANOVA results for F_z.

Source	DF	SS	MS	f-value	p-value	Contribution %
V_c	2	0.5489	0.2744	2.57	0.280	0.86
f	2	6.2974	3.1487	29.49	0.033	9.82
D	2	57.2989	28.6495	268.34	0.004	89.32
error	2	0.2135	0.1068			
total	8	64.3587				

Table 8

ANOVA results for M_z.

Source	DF	SS	MS	f-value	p-value	Contribution %
V_c	2	0.3282	0.16408	3.44	0.225	1.92
f	2	1.6496	0.82481	17.31	0.055	9.68
D	2	15.0675	7.53374	158.12	0.006	88.40
error	2	0.0953	0.04764			
total	8	17.1406				

Next, the f-value was used to determine the contribution percentage of the factors. The tool diameter D was found to have a contribution percentage equal to 89.32% on the produced thrust force and 88.4% on the torque respectively, proving that it is the most effective term. Feed rate contributes to the two output parameters with 9.8% and 9.7% accordingly. The strong fit of the models was highlighted by the predicted and the adjusted R-values, being 99.53% and 98.11% for F_z. The equivalent values were calculated equal to 99.44% and 97.78% for M_z. Specifically, the

adjusted and the predicted R-square pose an indication that the terms involved in the models are sufficient. Moreover, they suggest that the models can generate reliable output within the specified range of machining conditions.

To further validate the reliability of the models, three standard plots were prepared. The normal probability plot was plotted to check the normality assumption. Figure 3 depicts the plot, where it is shown that the errors are normally distributed across the fit line, without any extreme departure for both F_z (Figure 3a) and M_z (Figure 3b).

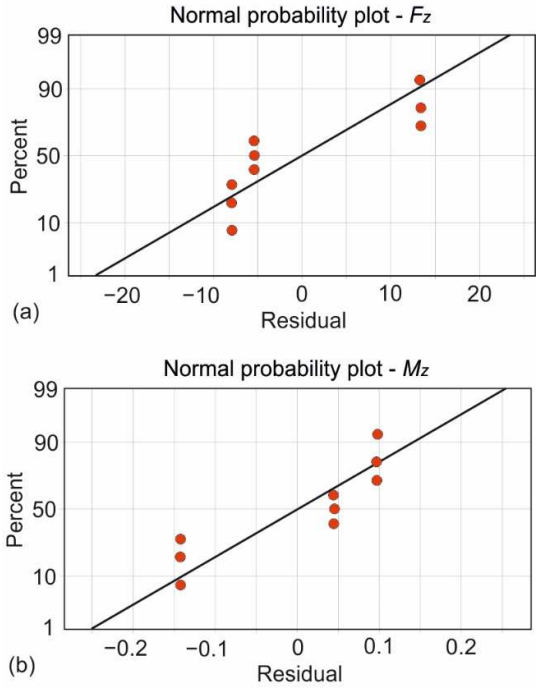

Fig.3. The normal probability plot for F_z (a) and M_z (b)

Figure 4 illustrates the residuals versus the fitted values. Specifically, Figure 4a shows that the residuals are independently distributed between the two sides of the chart. A similar pattern, with well spread points and no clustering, is identified in Figure 4b for the torque. Finally, Figure 5 depicts the plotting of the residuals in time order. With this plot the independence of the residual is checked. Both Figure 5a and 5b do not illustrate any obvious pattern, proving the validity of the experimental design.

3.3 Assessment of the variables effect

The main effects plots shown in Figure 6, were used for the visualization of the changes in the parameter mean values. Such plots are considered graphical tools, that facilitate the visualization of the effects generated by a number of factors [15]. Figure 6a and 6b illustrate the individual effect of each one of the three cutting factors, on the force and torque output respectively.

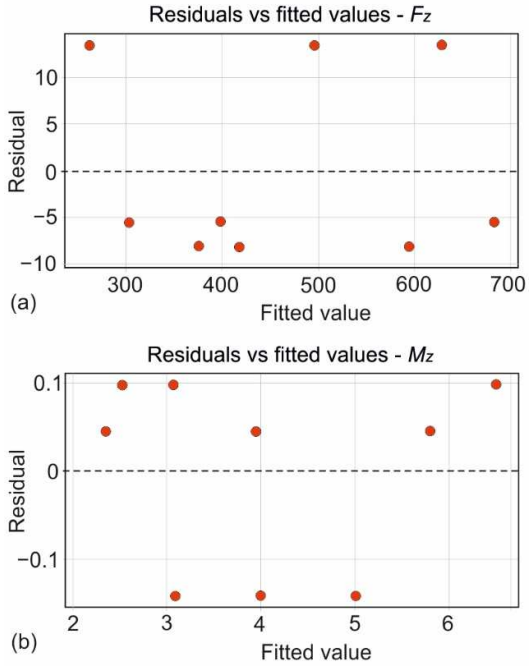

Fig.4. The residuals versus fits plots for F_z (a) and M_z (b)

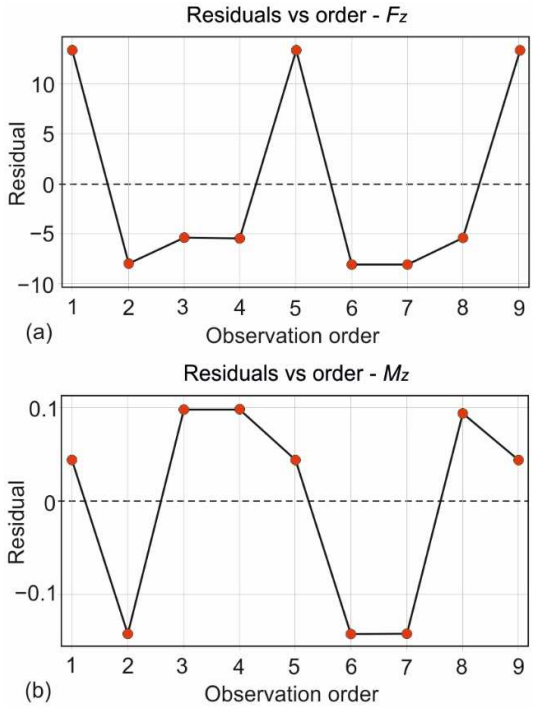

Fig.5. The residuals versus order plots for F_z (a) and M_z (b)

It is evident that the tool diameter acts increasingly for both output parameters. Especially the 12mm drill generates the most significant result. Feed rate follows a similar trend to the one presented by the tool diameter, but with milder increasing effect. Finally, the cutting speed seems to differentiate in terms of the effect pattern. Specifically, the increase in cutting speed leads to marginal increased force output. In contrast, the same increase, slightly decreases the torque value.

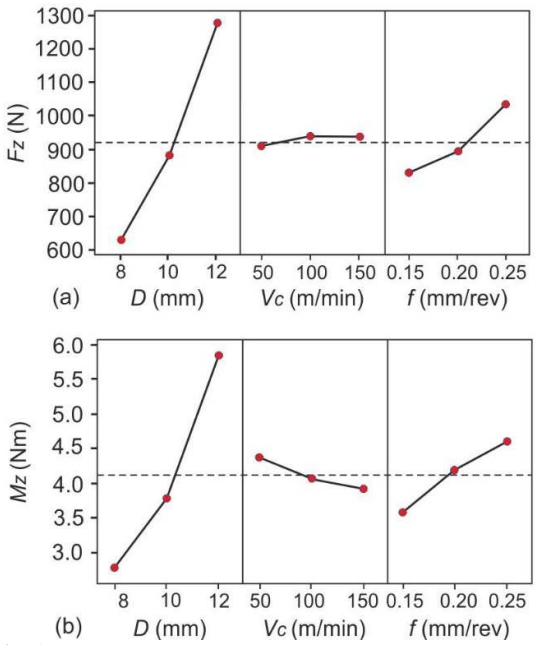

Fig.6. The main effects plot for means: F_z (a) and M_z (b)

3.4 Identification of optimal conditions

The main effects plots of the S/N ratios, revealed the ideal combinations of cutting factors, for minimizing the thrust force (Figure 7a) and cutting torque (Figure 7b) accordingly. The combinations were formed based on the factor levels that maximize the equivalent S/N ratio. Upon identifying the optimal parameter levels, they were used to predict the output parameters. Table 9 includes the optimal cutting conditions for both output, as well as the predicted values compared to the experimental results. Since the tool size is the parameter that contributes the most to the model, it was expected that its S/N would be the highest compared to the other two terms. Consequently, the low relative error indicates a good level of agreement between the model and the experimental work.

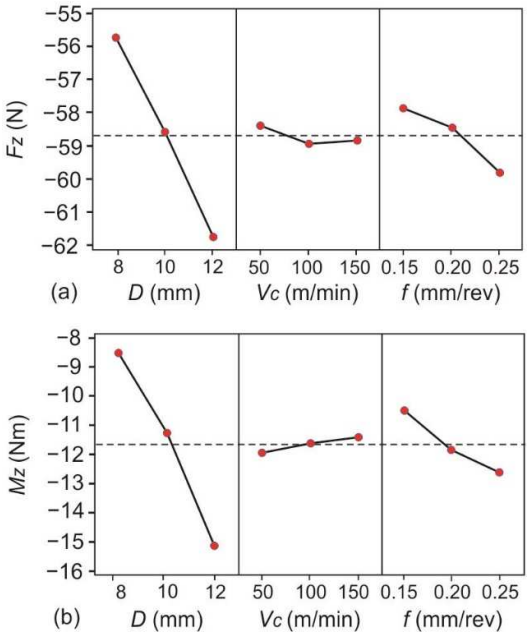

Fig.7. The main effects plot for S/N ratios: F_z (a) and M_z (b)

Table 9

Optimal parameter levels for thrust force and torque.

Optimal value					
V_c (m/min)	f (mm/rev)	D (mm)	Predicted output	Experiment	Relative error
50	0.15	8	F_z = 521.1 N	548.5 N	−5.00%
150	0.15	8	M_z = 1.90 Nm	2.16 Nm	−12.04%

To calculate the predicted optimal output values, Equation 2 was used. Where Y_{opt} is the predicted response after optimization. Therefore, for this study it denotes either F_z or M_z. $\bar{Y}$ is the mean value of the response for all experiments, thus 919.6N and 4.03Nm respectively. Finally, Y_i represents the best possible value of the response at each individual

factor, with n being the number of the factors. Hence, n would be equal to 3 for this study since the investigation factors are the cutting speed, the feed and the tool. Moreover, the best possible value for each response, would be the lowest value of thrust force and torque at each one of the aforementioned cutting parameters.

$$Y_{opt} = \overline{Y} + \sum_{i=1}^{n} \left(Y_i - \overline{Y} \right) \quad (2)$$

Equations 3 and 4 describe the calculations for the optimal responses according to the three terms, the mean value for each response and equation 2.

$$F_{z(opt)} = 919.6 + (903 - 919.6) + (833 - 919.6) + (624.3 - 919.6) = 521.1\,\text{N} \quad (3)$$

$$M_{z(opt)} = 4.03 + (3.83 - 4.03) + (3.47 - 4.03) + (2.66 - 4.03) = 1.90\,\text{N} \quad (4)$$

4. CONCLUSION

In the present study, the Taguchi method was utilized to identify the control factors of the AA6082-T6 drilling with carbide tools. ANOVA results provided insight on the statistical significance of the factors, as well as the contribution level. The study revealed that the tool diameter affects the most both output parameters, acting increasingly as larger sizes are used. In addition, the feed rate seems to have a similar effect on the output. However, the magnitude is much lighter compared to the one induced by the drill size. The highest contribution percentages were identified to be 89.32% and 88.40%, corresponding to the tool diameter for both models. Concluding, the optimal cutting conditions were determined, that lead to the minimization of both the thrust force and the cutting torque. The corresponding values are V_c=50m/min, f=0.15mm/rev and D=8mm for F_z, and V_c=150m/min, f=0.15mm/rev and D=8mm for M_z. Finally, the graphical analysis of the results highlighted the high correlation between the experimental and the predicted results for both output factors, with prediction coefficient of determination equal to 98.11% for the F_z model and 97.78% for the M_z model accordingly.

Future work in the field, include the investigation of the machinability performance of aluminium-composite materials during drilling, as well as the evaluation of more advanced modeling techniques such as the FE method and the neural networks.

5. REFERENCES

[1]F. Veiga, A., Suárez, A.G. Del Val, M. Penalva and L.N.L. De Lacalle, *Evaluation on advantages of low frequency assisted drilling (LFAD) aluminium alloy Al7075*, Int. J. Mechatronics Manuf. Syst. 13 (2020), pp. 230–246.

[2]M. Kimmelmann, J., Duntschew, I. Schluchter and H.C. Möhring, *Analysis of burr formation mechanisms when drilling CFRP-aluminium stacks using acoustic emission*, Procedia Manuf. 40 (2019), pp. 64–69.

[3]A. Tzotzis, C., García-Hernández, J.-L. Huertas-Talón and P. Kyratsis, *FEM based mathematical modelling of thrust force during drilling of Al7075-T6*, Mech. Ind. 21 (2020), pp. 415.

[4]A. Bharatish, H.N., Narasimha Murthy, B., Anand, K.N. Subramanya, M. Krishna and P. V. Srihari, *Assessment of drilling characteristics of alumina coated on aluminium using CO2 laser*, Meas. J. Int. Meas. Confed. 100 (2017), pp. 164–175.

[5]J. Xiang, S., Pang, L., Xie, F., Gao, X,. Hu, J., Yi et al., *Mechanism-based FE simulation of toolwear in diamond drilling of SiCp/Al composites*, Materials (Basel). 11 (2018), .

[6]Tzotzis, A., Markopoulos, A.P., Karkalos, N.E., Tzetzis, D., Kyratsis, P. FEM based investigation on thrust force and torque during Al7075-T6 drilling, in IOP Conference Series: Materials Science and Engineering, 1037 (2021), pp. 012009.

[7]Tzotzis, A., Markopoulos, A., Karkalos, N., .

Kyratsis, P. 3D finite element analysis of Al7075-T6 drilling with coated solid tooling, in MATEC Web of Conferences, 318 (2020), pp. 1–6.

[8]Kyratsis, P., Tzotzis, A., Davim, J.P. *Experimental and 3D Numerical Study of AA7075-T6 Drilling Process*, in *3D FEA Simulations in Machining*, Springer International Publishing, Cham, 2023, pp. 63–75.

[9]Jebarose S., Prakash, J. *Optimization of burr height in drilling of aluminium matrix composites (LM5/ZrO2) using Taguchi technique*, Adv. Mater. Process. Technol. 8 (2022), pp. 417–426.

[10] Kamaraj, M., Santhanakrishnan, R., Muthu, E. *Investigation of surface roughness and MRR in drilling of Al2O3 particle and sisal fibre reinforced epoxy composites using TOPSIS based Taguchi method*, IOP Conf. Ser. Mater. Sci. Eng. 402 (2018), .

[11] Saravanan, V., Francis Xavier, V., Sudeshkumar, M.P., Maridurai, T., Suyamburajan, V., Jayaseelan, V. *Optimization of SiC Abrasive Parameters on Machining of Ti-6Al-4V Alloy in AJM Using Taguchi-Grey Relational Method*, Silicon 14 (2022), pp. 997–1004.

[12] Ramesh, S., Viswanathan, R., Ambika, S. *Measurement and optimization of surface roughness and tool wear via grey relational analysis, TOPSIS and RSA techniques*, Meas. J. Int. Meas. Confed. 78 (2016), pp. 63–72.

[13] Kyratsis, P., Tzotzis, A., Markopoulos, A., Tapoglou, N. *CAD-Based 3D-FE Modelling of AISI-D3 Turning with Ceramic Tooling*, Machines 9 (2021), pp. 4.

[14] Kao, J.Y., Hsu, C.Y., Tsao, C.C. *Experimental study of inverted drilling Al-7075 alloy*, Int. J. Adv. Manuf. Technol. 102 (2019), pp. 3519–3529.

[15] Tzotzis, A., Kakoulis, K., Efkolidis, N., Kyratsis, P. *Acta technica napocensis*, ACTA Tech. NAPOCENSIS-Series Appl. Math. Mech. Eng. 65 (2022), pp. 1417–1424.

Cercetarea experimentală și analiză Taguchi privind parametrii de găurire pentru aliajul structural de aluminiu

Găurirea aliajelor structurale de aluminiu (AA) este unul dintre cele mai frecvent aplicate procese în industrie. Acest studiu utilizează o matrice ortogonală Taguchi L9, pentru a investiga influența a trei parametri cheie de prelucrare (viteza de așchiere, avansul și diametrul sculei), asupra forțelor de așchiere și a cuplului de tăiere induse în timpul găuririi aliajului Al6082 T6. Cele 9 experimente au fost efectuate pe o mașină CNC, în timp ce puterea dorită a fost măsurată cu un dinamometru rotativ. În plus, a fost utilizat un sistem de achiziție de date pentru a facilita colectarea datelor de ieșire. Analiza a relevat că diametrul sculei, urmat de avans sunt variabilele care afectează cel mai mult, ambii parametrii de ieșire. Mai mult, au fost identificate condițiile optime de tăiere, ținând cont de minimizarea forțelor de tăiere.

Anastasios TZOTZIS, PhD Post-Doctoral Researcher, University of Western Macedonia, Department of Product and Systems Design Engineering, a.tzotzis@uowm.gr

Nikolaos EFKOLIDIS, PhD Assistant Professor, University of Western Macedonia, Department of Product and Systems Design Engineering, nefkolidis@uowm.gr

Athanasios MANAVIS, PhD Post-Doctoral Researcher, University of Western Macedonia, Department of Product and Systems Design Engineering, manavis.athanasios@gmail.com

Panagiotis KYRATSIS, PhD Professor, University of Western Macedonia, Department of Product and Systems Design Engineering, pkyratsis@uowm.gr